

# Mixed Precision PointPillars for Efficient 3D Object Detection with TensorRT

1<sup>st</sup> Ninnart Fuengfusin

*Advanced Mobility Research Institute  
Kanazawa University  
Ichikawa, Japan*

ninnart@se.kanazawa-u.ac.jp

2<sup>nd</sup> Keisuke Yoneda

*Advanced Mobility Research Institute  
Kanazawa University  
Ichikawa, Japan*

k.yoneda@staff.kanazawa-u.ac.jp

3<sup>rd</sup> Naoki Suganuma

*Advanced Mobility Research Institute  
Kanazawa University  
Ichikawa, Japan*

suganuma@se.kanazawa-u.ac.jp

**Abstract**—LIDAR 3D object detection is one of the important tasks for autonomous vehicles. Ensuring that this task operates in real-time is crucial. Toward this, model quantization can be used to accelerate the runtime. However, directly applying model quantization often leads to performance degradation due to LIDAR’s wide numerical distributions and extreme outliers. To address the wide numerical distribution, we proposed a mixed precision framework designed for PointPillars. Our framework first searches for sensitive layers with post-training quantization (PTQ) by quantizing one layer at a time to 8-bit integer (INT8) and evaluating each model for average precision (AP). The top-k most sensitive layers are assigned as floating point (FP). Combinations of these layers are greedily searched to produce candidate mixed precision models, which are finalized with either PTQ or quantization-aware training (QAT). Furthermore, to handle outliers, we observe that using a very small number of calibration data reduces the likelihood of encountering outliers, thereby improving PTQ performance. Our methods provides mixed precision models without training in the PTQ pipeline, while our QAT pipeline achieves the performance competitive to FP models. With TensorRT deployment, our mixed precision models offer less latency by up to 2.538 times compared to FP32 models.

**Index Terms**—neural networks, quantization, 3D object detection

## I. INTRODUCTION

LIDAR 3D object detection has enabled autonomous cars to recognize the surrounding environment. To ensure that the task performs accurately and operates in real-time is crucial to success. However, autonomous cars are often equipped with edge devices with limited computing capacity and memory. Hence, the deployment of 3D object detection models has become the challenge.

Toward this, PointPillars [1] are promising candidate models due to their low runtime latency compared to other models, such as point-based models [2] and voxel-based models [3]. This is because PointPillars process 3D point cloud into 2D pseudo-images, which can be fed directly into 2D convolutions. This processing helps avoid the use of expensive 3D convolutions [3] and complex point sampling [4].

Furthermore, model quantization promises to reduce latency by constraining the expensive 32-bit floating point (FP32) to a lower bit-width datatype, such as 8-bit integer (INT8). This enables low-precision arithmetic that is faster and requires lower memory bandwidths.

To quantize a model, post-training quantization (PTQ) is attractive, compared to quantization aware training (QAT). Since PTQ does not require any training, it requires only a small set of data for calibration by performing forward propagations and tracking statistical information. However, directly applying PTQ INT8 quantization to PointPillars causes a dramatic performance drop [5]. QAT may reduce the performance drop from INT8 quantization; however, there is still a performance gap compared to the FP32 model, as shown in Table I.

TABLE I  
INT8 PTQ AND QAT WITH POINTPILLARS. THE MODELS WERE EVALUATED ON THE KITTI 3D OBJECT DETECTION DATASET [6]. THE 3D AVERAGE PRECISION OVER 11 AND 40 RECALL VALUES (AP11, AP40) ARE REPORTED OVER THREE DIFFICULTIES.

Data Type	Car AP11			Car AP40		
	Easy	Mod.	Hard	Easy	Mod.	Hard
FP32	<b>86.35</b>	<b>76.95</b>	<b>75.46</b>	<b>87.13</b>	<b>78.49</b>	<b>75.84</b>
PTQ INT8	27.29	23.63	20.18	25.35	21.43	18.66
QAT INT8	75.06	64.64	61.48	77.93	64.7	60.56

In this work, instead of introducing novel architectures [7] or quantization schemes [5], we propose using a mixed precision based method by quantizing less sensitive layers to INT8 and more sensitive layers to 16-bit floating points (FP16).

To find sensitive layers, PTQ is used to quantize one of layers to INT8 and evaluate the 3D average precision over 40 recall values (AP40). With PTQ, the sensitive search is performed without additional training. Layers with low AP40 scores are denoted as the high-sensitivity layers.

After sensitive layers are identified, a greedy search is used to discover combinations of INT8 sensitive layers to assign with the FP16 datatype. Finally, these layer combinations are calibrated again with either PTQ or QAT. With mixed precision and greedy search, we demonstrate that conventional quantization algorithms can operate without any modifications. The overview of these methods is visualized in Fig. 1

Furthermore, for PTQ, we observe that using a very small number of calibration data leads to better performance of models. This is because the fewer calibration samples used, the lower the chance of encountering extreme outliers. Therefore,

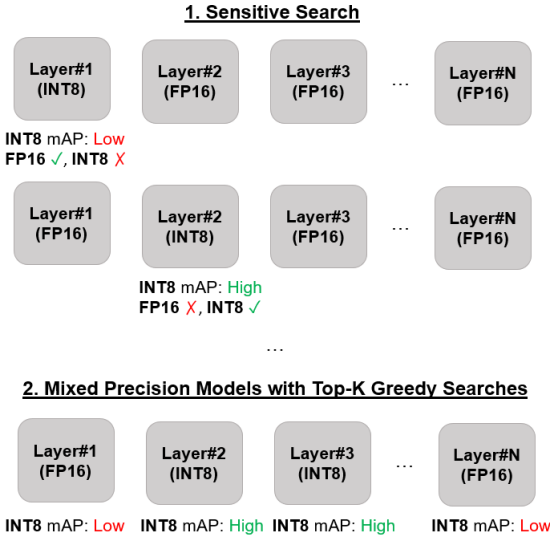


Fig. 1. Overview of our proposed method. First, sensitive layers are identified by quantizing one layer at a time to INT8 using PTQ. Second, a greedy search is used to discover mixed precision models where these sensitive layers are replaced with FP16 layers.

this reduces rounding errors due to wider quantization step sizes.

To ensure that our mixed precision models can be deployed, our method complies with TensorRT [8] requirements. We provide extensive evaluations of TensorRT’s runtime latency across two devices: Jetson Orin and RTX 4070Ti.

In this work, we focus on using only FP16 and INT8 datatypes due to their wide support across both old and modern hardware. With these approaches, our method aims to minimize AP40 loss from INT8 quantization while providing the lower runtime latency compared to other models.

To the best of our knowledge, our main contributions in this paper are listed as follows:

- We propose a mixed precision framework designed for PointPillars and TensorRT. Instead of using only latency as the metric, as commonly used with TensorRT, our method instead uses model performance to search for optimal layer combinations instead.
- Our framework uses PTQ to identify top- $k$  sensitive layers and utilizes greedy searches to find top- $k$  optimal combinations of mixed precision layers for further using with either PTQ or QAT.
- We observe a negative correlation between PTQ model performance and the number of calibration data. To enhance the performance of PTQ models, we propose using a very small number of calibration data to avoid extreme outliers.

## II. RELATED WORKS

In this section, we describe the related works that lie at the intersection between 3D object detection models and quantization.

Quantizing 3D object detection models is challenging due to high sparsity, extreme outliers, and wide numerical distributions [5], [7]. To perform PTQ on 3D object detection model, LIDAR-PTQ [5] was proposed with a new data calibration technique that accounts for the sparsity and introduces a loss function that minimizes the prediction differences between FP32 and INT8 models. With the extra-loss term, LIDAR-PTQ is in between PTQ and QAT, as it requires training to optimize quantization parameters such as scaling factors and zero points, while requiring only unlabeled data.

On the other hand, PillarHist [7] was proposed with a novel pillar encoder that stabilizes the numerical distribution of variables within the pillar encoder, thereby enhancing PointPillars robustness to INT8 quantization.

Stanisz *et al.* [9] demonstrated the use of QAT with a PyTorch quantization framework, brevitas [10] to quantize PointPillars with different fixed point data precision across sub-modules. With empirical experiments, Stanisz *et al.* identified a combination between 2-, 4-, 8-bit integer sub-modules that achieves a 16x lower memory consumption, while average precision is reduced by at most 9% across all classes.

Compared to previous works, our work addresses the same research problems as LIDAR-PTQ [5] and PillarHist [7]. However, our approach differs by using mixed precision models to handle numerical distribution stabilization and using a very small number of calibration data to handle extreme outliers.

For Stanisz *et al.* [9] work, our works differs in that, instead of manually searching for data precision across sub-modules, our works uses PTQ to find sensitive layers and assign the data precision with. For deployment, brevitas [10], which uses asymmetric quantization by default, may cause an incompatibility to TensorRT deployment, as TensorRT only supports symmetric quantization [8]. With TensorRT, the precision of ReLU outputs is reduced by half and this can cause greater losses compared to Stanisz *et al.*.

In terms of mixed precision, TensorRT supports a mixed precision scheme; however, it finds a layer combination that minimizes latency, whereas our proposed method focuses on maximizing model accuracy. Furthermore, we observed that to enable this scheme, all layers should first be quantized to INT8, allowing TensorRT to choose between INT8 and other datatypes. However, relying on this selection can lead to degradation in model accuracy due to accumulated quantization losses from all layers.

## III. PROPOSED METHOD

In this section, we first describe the prerequisites of PointPillars, INT8 quantization and then discuss our proposed methods, mixed precision PointPillars.

### A. Prerequisites

1) *PointPillars*: PointPillars [1] proposes a novel pillar encoder that processes 3D point clouds into vertical columns called pillars. These pillars are further processed with PointNet [2] and scattered into 2D pseudo-images. The 2D pseudo-images are fed into 2D convolutional neural network (CNN)

backbone, which produces features for bounding box prediction with the detection head.

Based on these processes, MMDetection3D [11] further decomposes PointPillars into five sub-modules: voxel encoder, middle encoder, backbone, neck, and bbox head. An overview of this architecture is shown in Fig. 1. The voxel encoder processes the 3D point cloud into pillars and further encodes them using PointNet. The middle encoder scatters the voxel encoder output into 2D pseudo-images. The backbone processes these pseudo-images with 2D CNN, and the neck aggregates multi-scale features, which are then consumed by the bbox head to produce the 3D bounding boxes prediction.

2) *INT8 Quantization and TensorRT*: INT8 quantization is formulated as the affine transformation in (1), which maps a floating point value,  $x$  to its corresponding integer value,  $x_q$ . Here,  $\lfloor \cdot \rceil$  denotes rounding half to even and the  $\text{clamp}(x, q_{\min}, q_{\max})$  function clips  $x$  values to the range of  $[q_{\min}, q_{\max}]$ .

$$x_q = \text{clamp}\left(\lfloor \frac{x}{s} \rceil + z, q_{\min}, q_{\max}\right) \quad (1)$$

To comply with TensorRT requirements [8] that supports only symmetric quantization, we set  $z = 0$ ,  $q_{\min} = -128$ , and  $q_{\max} = 127$  for INT8 quantization. Therefore, (1) becomes (2).

$$x_q = \text{clamp}\left(\lfloor \frac{x}{s} \rceil, q_{\min}, q_{\max}\right) \quad (2)$$

For PTQ, min-max calibration provides better performance compared to entropy calibration for the LIDAR 3D object detection task [5]. Therefore, the min-max calibration is chosen and used to solve for  $s$  by (3), where  $x_{\min}$  and  $x_{\max}$  are the minimum and maximum values observed during data calibration.

$$s = \frac{\max(\text{abs}(x_{\min}), \text{abs}(x_{\max}))}{127} \quad (3)$$

## B. Mixed Precision PointPillars

In this section, we describe our proposed method, mixed precision PointPillars. We first describe how to discover sensitive layers and how to find suitable layer combinations for mixed precision models to use with final PTQ and QAT. After that, we discuss the concept behind our proposed method design, such as PointPillars latency for each layer across datatype and the correlation between the number of calibration data and model performance.

1) *PTQ Sensitive Layer Search*: To identify sensitive layers, PTQ is performed by quantizing one layer at a time to INT8 and evaluating for AP40. Then, the top- $k$  sensitive layers are selected to generate layer combinations for the candidate model.

To formalize, let  $D_{\text{train}}$ ,  $D_{\text{val}}$ , and  $D_{\text{cal}}$  denote the training, validation, and calibration datasets, respectively, where  $D_{\text{cal}} \subseteq D_{\text{train}}$ . Let the 3D average precision metric be defined as the function of  $AP40 : (\theta, D_{\text{val}}) \rightarrow \mathbb{R}$ .

To measure sensitivity, we construct the partially quantized model  $\theta^l$  with a single  $l$ -th INT8 layer created by PTQ, using  $D_{\text{cal}}$ . Our objective is to search for top- $k$  layers that yield the lowest validation performance. This statement is formulated as (4), where  $\mathcal{L} = \{1, \dots, L\}$  is the set of all layer indices and  $S$  is the set of top- $k$  sensitive layer indices.

$$S^* = \arg \min_{S \subseteq \mathcal{L}, |S|=k} \sum_{l \in S} AP40(\theta^l, D_{\text{val}}). \quad (4)$$

After top- $k$  sensitive layers  $S^*$  are found by searching across layers, with PTQ, this process does not require a significant amount of time. However, to find the most optimal combination of layers requires  $\binom{L}{k} = \frac{L!}{k!(L-k)!}$  combinations to search. With large  $L$ , this becomes combinatorially expensive.

To address this issue, we adopt a greedy search by ranking the most sensitive layers from the most to the least sensitive. Then, we construct candidate models by selecting the top-1 to top- $k$  sensitive layers to assign as the FP16 layers of the INT8 models. With this approach, only  $k$  combinations are required for the search.

After the search, once the candidate mixed precision models are found, we perform the final PTQ or QAT to calibrate or train the mixed precision models. With the sensitive layers replaced, our models can perform without issues caused by sensitive layers.

2) *INT8 and Latency*: To minimize latency, our proposed method is designed based on the promise that INT8 models deliver lower runtime compared to other datatypes. Therefore, by ensuring that almost all layers are INT8 and only a few sensitive layers are FP16, the overall latency of PointPillars model can be minimized.

To validate this statement, we convert PointPillars models to FP32, FP16, and INT8 with `trtexec`, a command line tool to TensorRT [8]. With this, we benchmarked the latencies across layers, as shown in Table IV.

From the table, in general, almost all INT8 layers promise a faster runtime compared FP32 and FP16 layers. Therefore, in terms of individual layer, INT8 layers provide lower runtime than FP32 and FP16 layers.

3) *Data Calibration and Performance*: LIDAR data is highly sparse and exhibits wide numerical distributions [5]. These properties often result in extreme outliers or values with large magnitude. In min-max calibration, these outliers determine  $x_{\max}$ , causing the  $s$  scaling factor or step size in (3) to increase. Consequently, the rounding error increases while the clipping error decreases.

For PTQ, we observe that using a very small number of calibration samples,  $|D_{\text{cal}}| \ll |D_{\text{train}}|$  (e.g. four input frames), reduces the chance of encountering extreme outliers, as demonstrated on the right side of Fig. 2. This demonstrates a positive correlation between the maximum observed input value and the number of calibration samples.

On the left side of Fig. 2, INT8 PointPillars with the first layer kept as FP32 is used to demonstrate a negative correlation between the mean 3D AP40 across three classes with moderate difficulty (mAP) and the number of data calibration

TABLE II

LATENCY FOR EACH WEIGHT LAYER WITHIN POINTPILLARS ACROSS THREE DATATYPES ON THE TO JETSON ORIN. EACH LAYER IS FUSED WITH ITS CORRESPONDING BATCH NORMALIZATION AND RELU.

Index	Layer Name	Latency (ms)		
		FP32	FP16	INT8
1	voxel_encoder.pfn_layers.0.linear	0.8624	<b>0.8542</b>	0.8655
2	backbone.blocks.0.0	1.382	0.5614	<b>0.3759</b>
3	backbone.blocks.0.3	1.369	0.5586	<b>0.3667</b>
4	backbone.blocks.0.6	1.369	0.5551	<b>0.3663</b>
5	backbone.blocks.0.9	1.369	0.5548	<b>0.3661</b>
6	backbone.blocks.1.0	0.6487	0.3045	<b>0.2454</b>
7	backbone.blocks.1.3	1.014	0.4941	<b>0.1749</b>
8	backbone.blocks.1.6	1.011	0.4926	<b>0.2771</b>
9	backbone.blocks.1.9	1.01	0.4925	<b>0.276</b>
10	backbone.blocks.1.12	1.011	0.4915	<b>0.2762</b>
11	backbone.blocks.1.15	1.011	0.4926	<b>0.2759</b>
12	backbone.blocks.2.0	0.5441	<b>0.2559</b>	0.2764
13	backbone.blocks.2.3	0.9886	0.4695	<b>0.4104</b>
14	backbone.blocks.2.6	0.9879	0.4688	<b>0.1483</b>
15	backbone.blocks.2.9	0.9894	0.4687	<b>0.2554</b>
16	backbone.blocks.2.12	0.9874	0.4696	<b>0.2552</b>
17	backbone.blocks.2.15	0.9882	0.4694	<b>0.2553</b>
18	neck.deblocks.0.0	0.6957	0.3634	<b>0.2553</b>
19	neck.deblocks.1.0	1.051	0.5117	<b>0.2553</b>
20	neck.deblocks.2.0	1.666	0.7109	<b>0.5723</b>
21	bbox_head.conv_dir_cls	0.9324	0.3979	<b>0.2423</b>
22	bbox_head.conv_reg	0.9781	<b>0.4527</b>	0.4807
23	bbox_head.conv_cls	0.7473	0.4082	<b>0.2545</b>

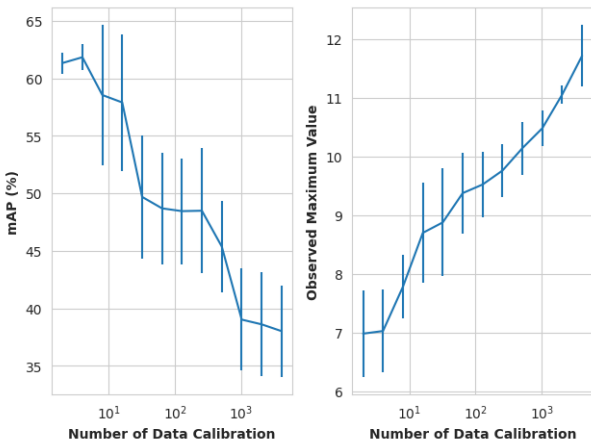


Fig. 2. Error bars indicate mean and standard deviation across five random seeds. **Left:** The relationship between the mean of 3D AP40 across three classes with moderate difficulty (mAP) and the number of data calibration samples. **Right:** The relationship between the maximum observed input value in the first convolutional layer of PointPillars and the number of data calibration samples. Note that the x-axis is provided in log scale.

samples. This indicates that PointPillars is more sensitive to rounding error than clipping error. The difference in mAP between four input frames and 4,096 frames is 23.82%. Therefore, throughout this work, only four input frames are used for the PTQ data calibration.

#### IV. EXPERIMENTAL RESULTS AND DISCUSSION

In this section, to demonstrate our proposed method, we conducted experiments with KITTI 3D object detection dataset [6]. MMDetection3D [11] was used to train and evaluate our PointPillars models. The default training setting of MMDetection3D for PointPillars was used, with the exception that the learning rate for QAT was adjusted to  $2 \times 10^{-4}$ . Additionally, to ensure similar behaviors between MMDetection3D and TensorRT, legacy option for voxel\_encoder was set to False.

To comply with TensorRT quantization schemes, we used modelopt [12] version 0.39.0 to perform PTQ and QAT. modelopt was slightly modified to support mixed precision models. FP32 pre-trained weights were used for the weight initialization for both PTQ and QAT. To convert the PointPillars model to TensorRT, we first converted our PyTorch [13] models to ONNX [14] and then converted the ONNX files to a TensorRT engine files using trtexec. We used two TensorRT version 10.13.2.6 for RTX 4070Ti and 10.3.0 for Jetson Orin.

##### A. Sensitive Layer Search

To find the sensitivity of each layer, the pre-trained FP32 model was used as the base model. Layer by layer, the layer within the base FP32 model was replaced with the corresponding INT8 layer. Then, this model was calibrated with PTQ using four randomly selected LIDAR frames from the training dataset and evaluated on the validation dataset.

To ensure that the sensitive layer search operates robustly across objects, the mAP was used as the main metric. The results are visualized as shown in Fig. 3

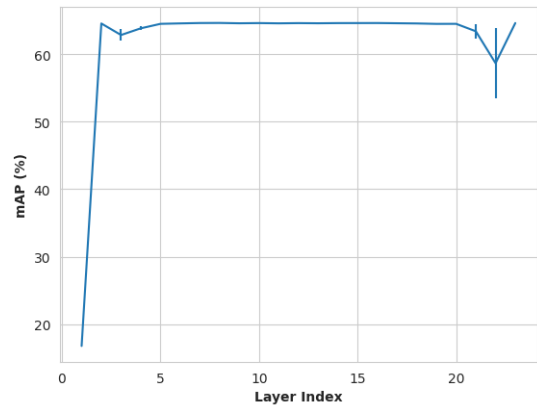


Fig. 3. Sensitive layer searches conducted across five random seeds, where errors bars indicate standard deviation. Y-axis indicates mAP. x-axis displays the layer index to assign as INT8 layer, where all other layers are FP32.

From the figure, the top-3 most sensitive layers with the lowest mAP after INT8 conversion are voxel\_encoder.pfn\_layers.0.linear, bbox\_head.conv\_reg, and backbone.blocks.0.3. The indices of these layers are 1, 22, and 3, as shown in Table IV. These layers were chosen as the target layers for the mixed precision model.

### B. Mixed Precision with PTQ and QAT

After the sensitive layers were identified with PTQ, the top- $k$  most sensitive layers were selected to construct layer combinations for mixed precision models. We found that only  $k = 3$  is sufficient to provide the model performance close to the FP32 model. Using a greedy search, top-1 to top-3 layers were used to create mixed precision models. Subsequently, these mixed precision models were either re-calibrated again with PTQ or trained with QAT to minimize the performance degradation.

For the notation of our mixed precision models, most layers are quantized to INT8, hence only a few FP16 layers require to be described. Therefore, our notation of "FP16: x,y" is used to describe a model with  $x$ -th and  $y$ -th as FP16 layers and all other layers are INT8 layers.

After tuning the mixed precision models with either PTQ or QAT, the performances of our models after TensorRT conversion are shown in Table III.

With mixed precision layers and a very small number of data calibration, our mixed precision PTQ models enhance the performance of the baseline PTQ model, "PTQ INT8". By assigning only one sensitive layer to FP16 with PTQ, "PTQ FP16: 1" outperforms "PTQ INT8" with mAP of 48.24%.

In Table III, there is a trend where replacing more sensitive layers with FP16 reduces performance degradation. Even without retraining, "PTQ FP16: 1,22,3" approaches the FP32 model, achieving an mAP of 63.84%, while "QAT FP16: 1,22,3" provides an mAP of 64.47%.

Furthermore, QAT provides an improvement over PTQ, ensuring a smaller performance gap between QAT and FP32. For instance, when comparing "PTQ FP16: 1,22,3" and "QAT FP16: 1,22,3", QAT provides an mAP improvement of 0.63% over PTQ and is only 0.17% lower than the FP32 model.

### C. Runtime Latency

In this section, we used `trtexec` to benchmark the runtime of our TensorRT models, as shown in Table IV.

Our model provides lower latency than other models with "FP16: 1", and compared to the FP32 model, "FP16: 1" reduces latency by a factor of 2.538 on the RTX4070Ti. However, adding more FP16 layers results in higher latency. We attribute this to the additional quantization and dequantization are required to convert between FP16 and INT8 datatypes. However, with RTX 4070Ti, this issue becomes less significant, as "FP16: 1,22,3" with three FP16 layers still provides lower latency than FP16 models.

### D. Correlations between Number of Calibration Samples and Easy and Hard Samples

We propose using a very small number of calibration samples to prioritize minimizing rounding error over the clipping error. While this improves overall performance, as shown in Fig. 2, it raises the question of whether this very small sample size will asymmetrically affect Hard samples (with smaller bounding boxes, higher occlusion levels and truncation) compared to Easy and Moderate samples or not.

We investigated this question by measuring the correlations between the number of calibration samples and mAP across three difficulty levels, as shown in Fig. 4, using the same settings as Fig. 2. The results show that the number of calibration samples exhibits a linear relationship with mAP across all difficulties, with a Pearson correlation for each level greater than 0.998. Therefore, the impact of reducing calibration samples is consistent across difficulty levels, suggesting this method remains robust in high-risk scenarios.

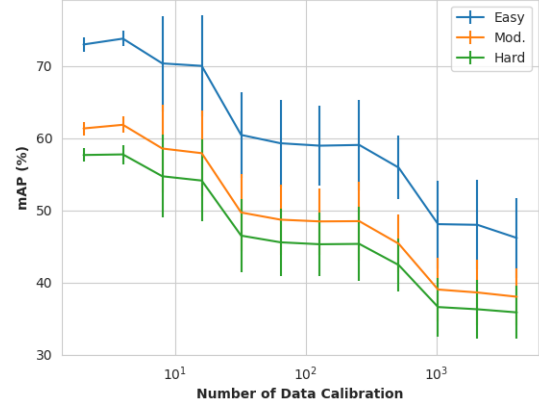


Fig. 4. The relationship between mAP and the number of data calibration samples across three difficulty levels.

## V. CONCLUSION

In this work, we proposed a mixed precision framework by assigning FP to sensitive layers, while other layers are assigned to INT8. Our framework discovers these sensitive layers by assigning one layer at a time to INT8 with PTQ and evaluating average precision. The top- $k$  layers with low average precision are assigned as the sensitive layers. Then, the sensitive layers are greedy searched to formulate candidate models for final PTQ or QAT.

With this framework, PTQ only pipeline promises competitive models without any training, and QAT pipeline achieves the performance equivalent to FP32 models. We also demonstrated that our models deliver lower latency compared to FP32 models by up to 2.538 times.

For future works, our works mainly support for FP32, FP16 and INT8 datatypes. We plan to extend our framework to other datatype supported by modern GPUs: 4-bit integer (INT4), 8-

TABLE III

PERFORMANCE OF BASELINE AND MIXED PRECISION MODELS WITH EITHER PTQ OR QAT. ALL MODELS WERE CONVERTED TO TENSORRT FORMAT AND EVALUATED FOR AP40.

Data Type	Car AP40			Cyclist AP40			Pedestrian AP40			mAP
	Easy	Moderate	Hard	Easy	Moderate	Hard	Easy	Moderate	Hard	
FP32	87.11	78.49	<b>75.84</b>	83.81	<b>64.89</b>	60.92	56.85	50.55	46.05	<b>64.64</b>
FP16	87.02	78.49	75.82	83.57	64.71	<b>61.03</b>	<b>56.98</b>	50.53	<b>46.22</b>	64.58
PTQ INT8	54.26	37.00	32.39	1.21	0.64	0.62	2.22	1.71	1.75	13.12
QAT INT8	83.25	72.32	67.70	78.28	56.82	53.35	51.47	45.58	42.03	58.24
PTQ FP16: 1	83.84	74.68	70.30	78.61	61.46	57.81	54.73	47.94	43.04	61.36
PTQ FP16: 1,22	87.29	75.34	70.48	81.20	60.88	57.09	56.07	50.42	46.04	62.21
PTQ FP16: 1,22,3	86.78	77.52	73.22	82.20	63.78	59.72	56.32	50.23	45.94	63.84
QAT FP16: 1	86.32	75.51	72.90	77.87	59.74	55.85	55.16	48.97	45.08	61.40
QAT FP16: 1,22	<b>87.55</b>	76.64	73.90	<b>83.92</b>	63.79	59.78	54.13	48.20	43.69	62.88
QAT FP16: 1,22,3	87.49	<b>78.58</b>	75.80	81.98	64.01	60.47	56.97	<b>50.83</b>	46.03	64.47

TABLE IV  
MEAN LATENCY PER DEVICES ACROSS DATATYPES

Data Type	Mean Latency (ms)	
	Jetson Orin	RTX 4070Ti
FP32	32.91	3.713
FP16	18.27	1.866
INT8	14.77	1.774
FP16: 1	<b>14.29</b>	<b>1.463</b>
FP16: 1,22	17.91	1.797
FP16: 1,22,3	18.40	1.837

bit floating point (FP8), and others. We also plan to extend this work to cover other 3D object detection models.

#### ACKNOWLEDGMENT

We appreciate all anonymous reviewers for their reviews and comments to improve this manuscript.

To enhance readability, all sections of this paper have been edited for grammar using ChatGPT 5 [15] and Gemini 3 [16].

This work was supported by Council for Science, Technology and Innovation (CSTI), Cross-ministerial Strategic Innovation Promotion Program (SIP) Phase 3, Construction of smart mobility platform, "Development of infrastructure and onboard sensor systems that utilize compact LiDAR technology to understand the actual situations of streets in living areas and busy districts" (funded by NEDO).

#### REFERENCES

- [1] A. H. Lang, S. Vora, H. Caesar, L. Zhou, J. Yang, and O. Beijbom, "Pointpillars: Fast encoders for object detection from point clouds," in *Proceedings of the IEEE/CVF conference on computer vision and pattern recognition*, 2019, pp. 12 697–12 705.
- [2] C. R. Qi, H. Su, K. Mo, and L. J. Guibas, "Pointnet: Deep learning on point sets for 3d classification and segmentation," in *Proceedings of the IEEE conference on computer vision and pattern recognition*, 2017, pp. 652–660.
- [3] Y. Zhou and O. Tuzel, "Voxelnet: End-to-end learning for point cloud based 3d object detection," in *Proceedings of the IEEE conference on computer vision and pattern recognition*, 2018, pp. 4490–4499.
- [4] C. R. Qi, L. Yi, H. Su, and L. J. Guibas, "Pointnet++: Deep hierarchical feature learning on point sets in a metric space," *Advances in neural information processing systems*, vol. 30, 2017.
- [5] S. Zhou, L. Li, X. Zhang, B. Zhang, S. Bai, M. Sun, Z. Zhao, X. Lu, and X. Chu, "Lidar-ptq: Post-training quantization for point cloud 3d object detection," *arXiv preprint arXiv:2401.15865*, 2024.
- [6] A. Geiger, P. Lenz, and R. Urtasun, "Are we ready for autonomous driving? the kitti vision benchmark suite," in *2012 IEEE conference on computer vision and pattern recognition*. IEEE, 2012, pp. 3354–3361.
- [7] S. Zhou, Z. Yuan, D. Yang, X. Hu, J. Qian, and Z. Zhao, "Pillarhist: A quantization-aware pillar feature encoder based on height-aware histogram," in *Proceedings of the Computer Vision and Pattern Recognition Conference*, 2025, pp. 27 336–27 345.
- [8] NVIDIA Corporation, *NVIDIA TensorRT Documentation*, 2025, accessed: 2025-11-6. [Online]. Available: <https://docs.nvidia.com/deeplearning/tensorrt/latest/index.html>
- [9] J. Stanisz, K. Lis, T. Kryjak, and M. Gorgon, "Optimisation of the pointpillars network for 3d object detection in point clouds," in *2020 Signal Processing: Algorithms, Architectures, Arrangements, and Applications (SPA)*. IEEE, 2020, pp. 122–127.
- [10] G. Franco, A. Pappalardo, and N. J. Fraser, "Xilinx/brevitas," 2025. [Online]. Available: <https://doi.org/10.5281/zenodo.3333552>
- [11] M. Contributors, "MMDetection3D: OpenMMLab next-generation platform for general 3D object detection," <https://github.com/open-mmlab/mmdetection3d>, 2020.
- [12] N. Corporation, *TensorRT Model Optimizer (ModelOpt)*, 2025, accessed: 2025-11-6. [Online]. Available: <https://nvidia.github.io/TensorRT-Model-Optimizer/>
- [13] A. Paszke, S. Gross, F. Massa, A. Lerer, J. Bradbury, G. Chanan, T. Killeen, Z. Lin, N. Gimelshein, L. Antiga *et al.*, "Pytorch: An imperative style, high-performance deep learning library," *Advances in neural information processing systems*, vol. 32, 2019.
- [14] J. Bai, F. Lu, K. Zhang *et al.*, "Onnx: Open neural network exchange," <https://github.com/onnx/onnx>, 2019.
- [15] OpenAI, "ChatGPT 5," <https://chat.openai.com/>, (accessed Jan. 29, 2026).
- [16] Google, "Gemini 3," <https://gemini.google.com/>, (accessed Jan. 29, 2026).